into the electronic correlations. To reconcile all the existing measurements, a detailed knowledge of the low-energy electronic structure is needed. Until now, the study of the detailed electronic band structure of $LiTi_2O_4$ has been hindered by the lack of high-quality single crystals and high energy resolution. This chapter follows up on this and presents the three-dimensional band structure measured on thin films by ARPES.

5.2 Three-Dimensional Electronic Band Structure

The success in preparing high-quality epitaxial thin films of $LiTi_2O_4$ by PLD opens the opportunity to perform band structure measurements by ARPES. Even more importantly, the SIS beamline at the Paul Scherrer Institute in Switzerland provides users with a PLD system that can be connected to the ARPES endstation, making it possible to perform in situ measurements without exposure to air. This is important since $LiTi_2O_4$ is extremely air-sensitive, as mentioned above. With this technique, the electronic correlations can be probed in momentum space, offering vital information about the nature of this unique superconductor.

5.2.1 Methods

$LiTi_2O_4$ (111) thin films were grown in situ by PLD on Nb-doped $SrTiO_3$ (111) substrates. The Nb doping ensures that the substrate is metallic and thus that the sample is grounded to the ARPES endstation. The sample quality was characterized by RHEED to confirm a smooth two-dimensional surface condition; see Fig. 5.2a. Ultraviolet ARPES experiments were carried out at the SIS beamline at the Swiss Light Source. The sample temperature was approximately 20 K, unless stated otherwise. Photon energies ranged between 40 and 180 eV, with linear light polarizations perpendicular and parallel to the mirror plane indicated as LV and LH, respectively, following the notation of the previous chapters. The reciprocal space is indexed by k_z along the (111) direction and $k_{x,y}$ perpendicular in-plane to the (111) direction. Due to the high sensitivity of the sample, a fast degradation of the band structure upon photon irradiation was experienced. After one minute of irradiation, the bands broadened considerably, and after two minutes, they were merging with the background. This disappearance of the bands in the spectrum was irreversible, but did not result in any change in the XPS spectrum of the core levels, hinting towards local damage to the crystallinity rather than the dissipation of lithium. Therefore, high-statistics data were recorded by rasterizing the beam

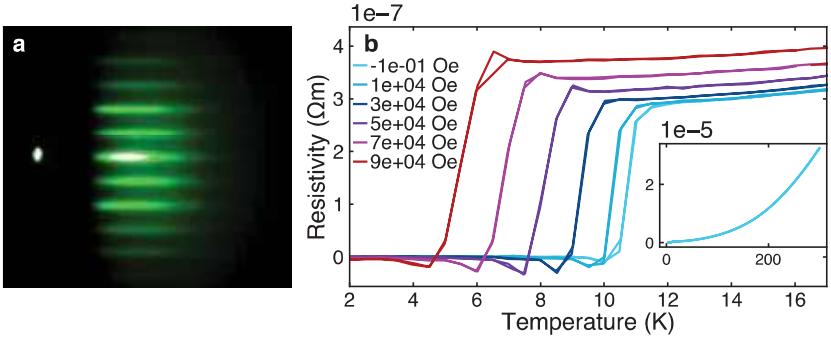

Figure 5.2: $LiTi_2O_4$. a RHEED pattern of $LiTi_2O_4$ (111) thin film grown by PLD. **b** Resistivity as a function of temperature, for different magnetic fields, measured on the thin film after the ARPES measurement. The inset shows the resistivity evolution up to 300 K.

over different sample spots. After the experiment, the superconducting transition temperature of 11 K was verified by a resistivity measurement; see Fig. 5.2b.

5.2.2 Results

An overview of the Fermi surface along the (111) direction in the normal state of $LiTi_2O_4$ is given in Fig. 5.3. The k_z dependence clearly shows the three-dimensional character of the Fermi surface with a periodic structure of pockets around the Γ points. The in-plane Fermi surface maps acquired with high photon energy, shown in Fig. 5.3b and c, give an overview of the 6-fold symmetric band structure expected for the (111) orientation. This confirms that the PLD-grown sample adapted to the substrate's (111) orientation.

The in-plane Brillouin zone boundary in this orientation can be inferred from the three-dimensional Brillouin zone shown in Fig. 5.3d. The Brillouin zone of an fcc lattice is a truncated octahedron, and adjacent zones are shifted in height compared to one another. The first Brillouin zone is shown on the right in the lower part of panel d, and the second zone to the left, shifted in height to connect two hexagonal faces. A horizontal cut through this structure therefore results in the zone boundaries indicated by solid black lines in panels b and c.

The evolution of the band structure at the Fermi level between the L and Γ points is shown in Fig. 5.4. At the L point, the Fermi surface is flower shaped with a weak pocket in the centre, which becomes larger and more pronounced with decreasing photon energy towards the Γ point. The flower-shaped feature gradually divides into six separated structures until they form necks at the corners of the hexagonal pocket

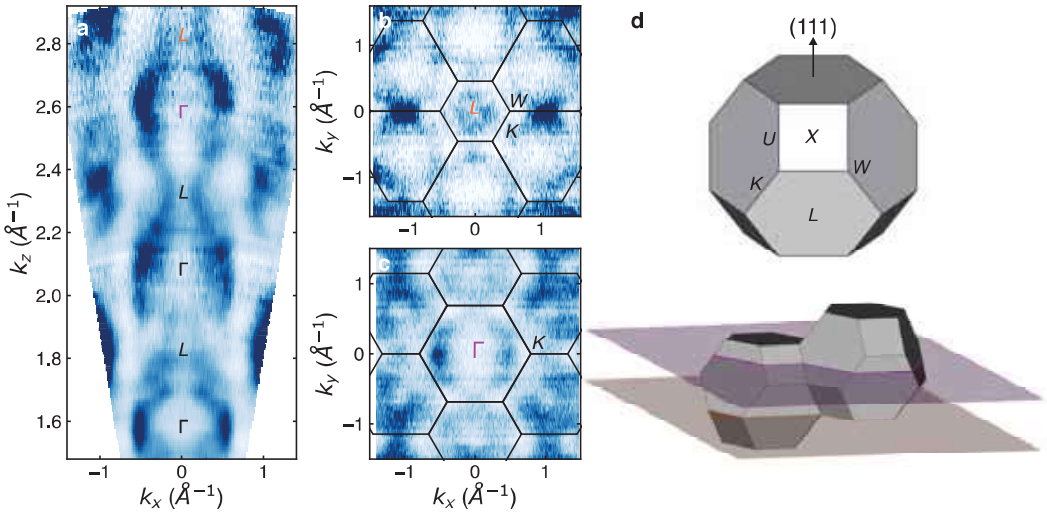

Figure 5.3: Three-dimensional band structure of $LiTi_2O_4$. **a** Out-of-plane Fermi surface covering more than three Brillouin zones. **b, c** In-plane Fermi surfaces recorded at photon energies cutting through the L and Γ points in the out-of-plane direction, respectively. Solid lines indicate zone boundaries. **d** Sketch of the Brillouin zone and in-plane cuts in **b, c**, neglecting the bending of the cuts due to fixed absolute momentum. Courtesy of P. Usai.

around Γ. In the following, the focus lies on the band structure recorded at 52 eV in the cut through Γ.

Energy distribution maps show the evolution of the electronic bands as a function of binding energy and are presented in Fig. 5.5 for cuts along the $\overline{\Gamma K}$ and approximately along the $\overline{\Gamma L}$ directions, with a 30° angle between them. It has to be noted that the $\overline{\Gamma L}$ cut with a constant k_z value does not cross the high-symmetry point L, since that is located at a different k_z value in the three-dimensional reciprocal space. Instead, the zone boundary following this cut is located between the L and U points. For simplicity, the cut is called $\overline{\Gamma L}$ nevertheless.

The comparison of LH and LV polarizations reveals only a weak polarization dependence. The LH data show more asymmetry with respect to the Γ point, with a weak and broad additional intensity below $-0.5\,\text{Å}^{-1}$ and above $0.5\,\text{Å}^{-1}$ that is strongest around -0.1 eV. The main band shows a broadening when probed with LH polarization compared with the LV polarization data. Most interestingly, the band in the cut $\overline{\Gamma K}$ shows strong correlation effects. The band has a kink around 50 meV and a pronounced broadening at higher energies. At Γ, the intensity is fully suppressed, but from higher photon energy measurements, the band bottom is visible at ~ 500 meV.

From the cut data in Fig. 5.5d, the correlation effects can be estimated by analysing

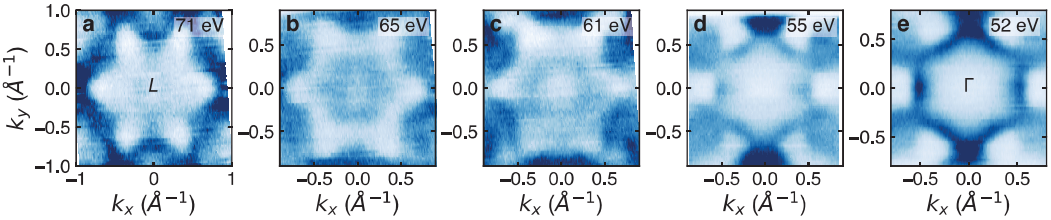

Figure 5.4: In-plane Fermi surfaces between Γ and L. a-e Fermi surface maps recorded with LV light polarization and photon energies as indicated.

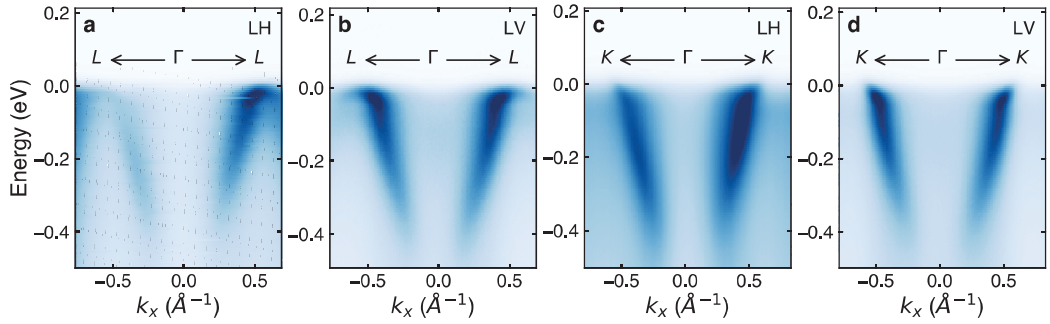

Figure 5.5: Band structure at Γ. a-d Raw data energy distribution maps recorded at 52 eV showing the band structure along the directions and recorded with light polarizations as indicated.

the MDCs and EDCs after subtracting a background EDC. The MDC analysis is summarized in Fig. 5.6 and shows initial signs of strong correlations. As explained in section 2.2, the ARPES intensity along an MDC assumes the form of a Lorentzian lineshape in the case of momentum-independent self-energy. For $LiTi_2O_4$, such a Lorentzian lineshape can be observed at higher binding energies in Fig. 5.6a, where a Lorentzian fit describes the data well. However, when approaching E_F, the MDC peak becomes increasingly asymmetric, and a Lorentzian fit no longer provides a good description of the data. There are several possible origins for such an asymmetry, for example a momentum-dependent self-energy, resolution effects or a contribution from another feature in the band structure. To extract the band dispersion, a different fitting approach is therefore required. To account for the asymmetry, the fitting function in Fig. 5.6b is composed of a constant background and a split Lorentzian function of the form

$$L(k, A, \Gamma_r, \Gamma_l, \mu) = \frac{2A}{\pi(\Gamma_l + \Gamma_r)} \left(\frac{\Gamma_l^2}{(k-\mu)^2 + \Gamma_l^2} \cdot \Theta(\mu - k) + \frac{\Gamma_r^2}{(k-\mu)^2 + \Gamma_r^2} \cdot \Theta(k - \mu) \right) \tag{5.1}$$

where Γ_l and Γ_r are the widths of the left and right side of the peak position μ, A is

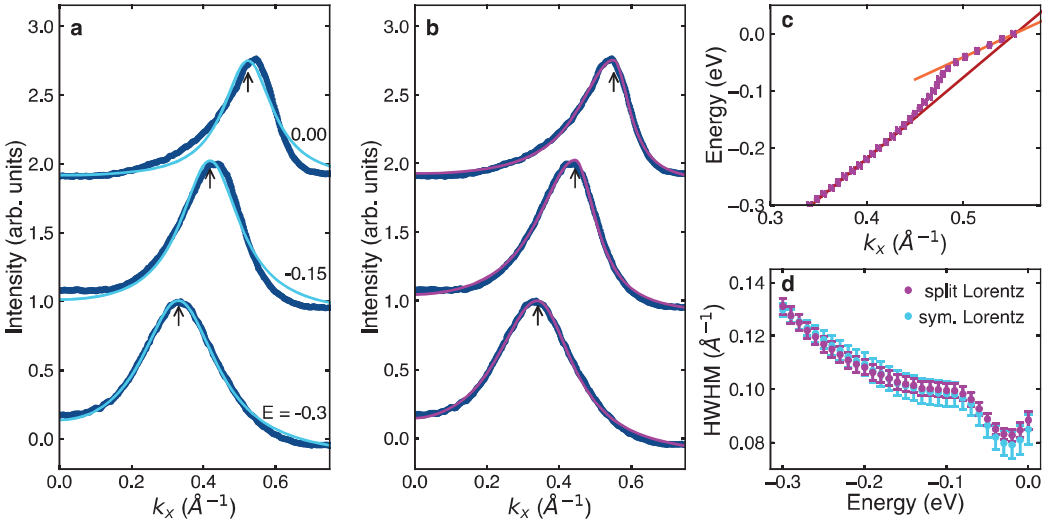

Figure 5.6: MDC analysis. **a, b** Example MDCs extracted from the energy distribution map in Fig. 5.5d at energies as indicated. Solid lines show a fit to the data composed of a Lorentz lineshape (**a**) or a split Lorentz lineshape (**b**) with a constant background. Black arrows denote the fitted peak position. **c** Band dispersion as extracted from peak positions in **b**. Solid lines show the fitted group velocities for the bare and renormalized quasiparticles. **d** Half-width-half-maximum (HWHM) extracted from fits in **a, b**. Error bars throughout the figure represent standard deviation from fitting.

the amplitude, Θ is the Heaviside function and the HWHM is given by $(\Gamma_l + \Gamma_r)/2$. This lineshape describes the data well across all binding energies and allows for precise tracking of the peak position. The extracted dispersion is shown in Fig. 5.6c and reveals the pronounced kink at 65 meV that was observed in the raw energy distribution map. This kink structure was measured outside the superconducting state at 20 K. With the MDC dispersion, it is possible to extract the bare and quasiparticle group velocities from the linear slope at high and low binding energies, respectively. Corresponding fits are shown in orange and red. Furthermore, the HWHM of the MDC peak can be inferred from the fit and is shown in Fig. 5.6d. Characteristically for a kink structure, the HWHM shows a step-like feature at the kink energy from the interaction. Interestingly, a second change in the behaviour of the HWHM can be observed at $\sim$ 150 meV, where the slope starts to increase again after a plateau around 100 meV. Comparing the two different fitting routines, with symmetric and split Lorentzian lineshapes, shows that the same behaviour of the HWHM is observed for both, indicating its robustness.

More information about the electronic band structure and the sign of correlations can be inferred from the EDC lineshape. Fig. 5.7a shows example EDCs extracted at different momenta. Around k_F, the typical peak–dip–hump structure is observed,

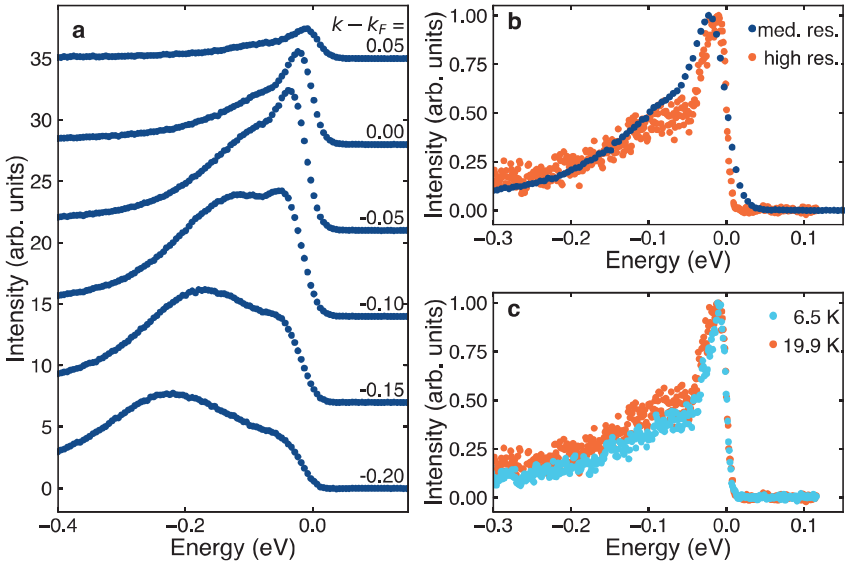

Figure 5.7: EDC analysis. **a** Example EDCs extracted from the energy distribution map in Fig. 5.5d at the indicated momenta. **b** Comparison of two EDCs extracted at k_F for two different energy resolutions, as indicated. **c** High-resolution EDCs at k_F for two different temperatures, as indicated.

which can be explained by the coherent and incoherent parts of the spectral function for interacting electrons. However, the dip is suppressed by the lack of sufficient energy resolution, as demonstrated in Fig. 5.7b, where a high-resolution spectrum reveals a more pronounced quasiparticle peak and subsequent dip.

A high resolution is therefore important in the analysis of the EDC lineshape. To gain insight into the superconducting state, the EDCs at k_F inside and outside the superconducting phase are compared in Fig. 5.7c. As expected, the opening of a gap is not observed, since the adopted energy resolution is not sufficient to detect a gap smaller than 2 meV [151, 160]. Interestingly, the overall shape of the EDC remains the same when crossing the superconducting transition, indicating that with the current resolution, no noticeable change in the low-energy electronic structure can be observed in the superconducting state.

5.2.3 Interpretation and Discussion

The observed kink feature, the peak–dip–hump structure and the step edge in the peak width are attributes of the interaction of quasiparticles with a bosonic mode. Indeed, in systems such as the cuprates, these features have been observed and analysed to extract the electron–phonon coupling λ [43, 161]. The electron–phonon coupling results in dressed electronic states, described by a quasiparticle peak close

to E_F with a mass renormalized by a factor $(1 + \lambda)$. The coupling can be extracted from the ratio of renormalized v_r and bare v_0 group velocities by [43, 161, 162]

$$\lambda = \frac{v_0}{v_r} - 1. \tag{5.2}$$

The velocities extracted from Fig. 5.6c are $v_0 = 1.42\,\mathrm{eV\,Å}$ and $v_r = 0.78\,\mathrm{eV\,Å}$, resulting in a coupling strength of $\lambda = 0.83 \pm 0.02$. This value is slightly higher than previously reported [163, 164], which could be indicative of a relevant electron–electron interaction. However, this result needs to be considered carefully, since the self-energy analysis of ARPES spectra is derived for two-dimensional systems with absent k_z dispersion and a momentum-independent self-energy. The former condition is not fulfilled by $LiTi_2O_4$, and the latter has to be questioned in light of the highly asymmetric lineshape in the MDC close to the Fermi level. A similar asymmetric shape has been observed for layered cobaltates [165], and has been attributed to a strong variation of the photoemission intensity with momentum.

Very recently, a preprint of an ARPES study on $LiTi_2O_4$ has been released [166]. The presented electronic band structure is in agreement with the results presented here, confirming the kink structure near the Fermi level. The temperature dependence of the kink revealed its formation at 150 K, defining a characteristic temperature for the electron–boson coupling. However, no sign of an energy gap opening or folding of the bands could be detected at that temperature. This result, combined with the absence of a change across the superconducting transition temperature presented here, suggests that the correlations play an important role in defining the intriguing electronic structure in $LiTi_2O_4$ over a broad temperature range.

Overall, the correlated electronic band structure presented here resembles what is found in the cuprates in many respects [43]. However, several distinct differences are observed. First, the MDC lineshape does not follow a simple Lorentzian, but is highly asymmetric close to E_F. Second, the HWHM, which is proportional to the imaginary part of the self-energy and therefore an indication of the quasiparticle lifetime, shows an additional change of trend above the kink energy. The value of the electron–boson coupling extracted here should be carefully put into perspective with the transition temperature and measurements of electron–phonon coupling performed using other techniques. Therefore, many open questions concerning the superconducting mechanism in $LiTi_2O_4$ remain, and higher energy resolution ARPES studies on high-quality films are necessary to confirm the superconducting gap symmetry.

5.2.4 Conclusions

The ARPES study on $LiTi_2O_4$ reveals its three-dimensional band structure and will therefore allow for a direct comparison of theory and measurements. Furthermore, the photon energy dependence allows for precise orientation within the bulk Fermi surface, identifying high-symmetry points. The cuts along high-symmetry directions reveal the strong electronic correlations present in this long-debated superconductor in the form of a pronounced kink structure, concomitant with a step edge in the peak width and the characteristic peak–dip–hump spectral lineshape. The analysis of this feature reveals a moderate electron–boson coupling. Future high-resolution measurements will be needed to gain insight into the superconducting energy gap symmetry and, with that, the elusive pairing mechanism.

6 Conclusions and Outlook

Quantum materials are deeply intriguing due to their useful emergent and tunable phases, like superconductivity, magnetic excitations and metal-to-insulator transitions. At the heart of these properties lie many-body systems composed of elementary particles, interactions and excitations, which often cannot be understood as isolated problems, but form part of a complex system. The various interactions between the elementary degrees of freedom, like the lattice, orbital, charge and spin degrees of freedom, result in a ground state from which different competing macroscopic phases can emerge. Unconventional superconductivity is found close to an antiferromagnetic insulating phase; however, other competing magnetic and electronic phases are usually present in the phase diagram too. An understanding of the macroscopic properties therefore requires knowledge of the microscopic interactions.

In this thesis, three projects on different quantum material families investigate such microscopic interactions in phases close to unconventional superconductivity.

In the ruthenate single-layer $Ca_{2-x}Sr_xRuO_4$, the system evolves from a Mott insulator to an unconventional superconductor by Sr substitution. Here, the focus is on the Ca side, where strong correlations lead to a magnetic insulating phase. The study of the low-energy excitation spectra in single-layer Ca_2RuO_4 and bilayer $Ca_3Ru_2O_7$ shows how the effective dimensionality and its different in-plane magnetic order results in fundamentally different excitation spectra. Furthermore, the extremely rich low-energy excitation spectrum in Ca_2RuO_4 is shown to be a result of the interplay between crystal-field splitting and spin–orbit coupling, and the lowest excitations exhibit a significant orbital character. The probing of such an excitation spectrum therefore allows for a determination of the spin–orbit coupling and provides valuable insights into the energy levels set by Coulomb interaction, Hund's coupling, crystal-field splitting and spin–orbit coupling.

Another compound family within the perovskite crystal lattice compounds that exhibit unconventional superconductivity are the famous high-temperature cuprate superconductors. Here, the La-based hole-doped cuprates have been investigated by RIXS to track the charge order phase, which is adjacent to and competes with superconductivity. The sensitivity of RIXS allows to the charge order to be tracked to high temperatures above the pseudogap phase and up to optimal doping, whereas

weaker charge correlations persist up to the highest doping levels measured. This result contributes to a long debate about the extent of charge order and its connection to superconductivity and the pseudogap phase. In addition, measuring phonon modes by RIXS allows extraction of the momentum-dependent electron–phonon coupling and its connection to charge order. It was shown that an electron–phonon coupling enhancement triggers a lock-in of the charge stripes. The interaction between the electronic and lattice degrees of freedom therefore has a direct impact on the charge order phase, and may also have implications for superconductivity.

The spinel superconductor $LiTi_2O_4$ was first believed to be a conventional *s*-wave superconductor, but recent evidence has pointed to an anomalous superconducting mechanism, and several parallels to cuprates have been drawn. With the ARPES study presented in this thesis, the three-dimensional band structure in the normal state is revealed, showing strong correlation effects. The kink structure allows for the extraction of a moderate electron–boson coupling, which is a key parameter in the formation of conventional Cooper pairing. These results, therefore, contribute to the determination of the relevant energy scales responsible for superconductivity and add crucial information to the debate around the pairing mechanism in this compound.

In summary, the presented projects present an experimental investigation of electronic interactions in correlated materials close to unconventional superconductivity or, in the case of $LiTi_2O_4$, the debated superconducting mechanism. It was possible to infer useful information about interactions like the spin–orbit coupling and the electron–phonon interaction. This contributes specific pieces to the larger puzzle of understanding the microscopic mechanisms in these materials, which will require a more holistic approach combining several experimental and theoretical approaches.

For example, the improved energy resolution in RIXS allows for a more detailed analysis of the excitation spectrum in Ca_2RuO_4, revealing a set of excitations and a dispersive behaviour for several of them. This challenges the theoretical model, which has been extended to a larger cluster size to compare it with the experimental results. However, the model would need a much larger cluster size or a different approach to capture a delocalized nature and dispersions. On the other hand, the resolution of RIXS is still limited compared to other techniques like neutron scattering. A further improvement is likely to reveal even more details in the excitation spectrum, e.g. in the excitation sector around 350 meV or the dispersion of the 40 meV mode.

Similarly, an improvement in resolution will benefit the understanding of the charge order phase and electron–phonon interaction in the cuprates. So far, only the bond-stretching phonon was resolved; the observation of lower-lying phonon modes with RIXS will allow for a more complete picture of the electron–phonon coupling, as

further modes might have a considerable effect on charge order via electron–phonon coupling. Concerning the charge order signal itself, future studies could focus on measuring the higher doping levels or, with improved resolution, confirm the possible dynamical nature of the weak charge correlations.

In $LiTi_2O_4$, the experimental investigation of the electronic band structure has just begun. So far, the study has been limited to the (111) orientation of the crystal lattice, leaving other termination planes untouched. Additionally, the current energy resolution is not sufficient to directly extract the superconducting gap from the spectrum, leaving the question about the pairing symmetry open. The role of the phonon modes in superconductivity is also still debated, and a combination of different experimental approaches is needed to gain further insight. Future developments in thin-film and single-crystal growth could also help the experimental efforts to resolve the many open questions about superconductivity in $LiTi_2O_4$.

In addition to these considerations closely related to the presented projects, the scope can be broadened by including the studies in surrounding phases, additional tuning parameters like strain or the effect of heterostructures. Moreover, new materials are being designed, not only in the search for a room-temperature superconductor, but also for the development of new technologies like spintronics and optoelectronics.

Concerning superconductivity, most discoveries are made by serendipity, rather than by design. So far, no clear recipe has been established for developing superconducting materials, and the known superconductors show wide variations in crystal structure and elemental composition. In unconventional superconductors, a layered structure is often found; however, the electronic correlations are influenced strongly by the detailed atomic arrangement. One would need to fully understand all present interactions and their interplay, and with this the organizing principles of complex phase diagrams, which represents a major intellectual challenge. Effort have also been made to find new superconductors by computational means [167]. On the experimental side, improvements in techniques are providing increasingly detailed insight into the electronic correlations. Several European synchrotrons are now upgrading to a new generation, which will lead to higher brilliance and coherence. Together with improvements in optics and detectors, this could help to reach higher energy resolutions in spectroscopic techniques without loss of flux. Experimental improvements will provide new valuable input for theoretical models and vice versa. In a completely different direction, deeper insight can be gained by studying dynamics with time-resolved techniques. Researchers on this frontier have been awarded this year's Nobel Prize "for experimental methods that generate attosecond pulses of light for the study of electron dynamics in matter" [168]. With attosecond techniques, our current understanding of electron dynamics will be challenged, as we will be able to probe beyond broadly adopted simplifications like the sudden approximation.

Altogether, the central challenge is to relate all experimental and theoretical findings to one another and to keep the overall picture in mind. The study of strongly correlated quantum materials is a complex field of research and involves exploring a wide variety of electronic and magnetic phenomena. Although great effort has been put into the understanding of these materials, there is still much to learn.

7 Acknowledgements

The last four years have been an adventurous journey in which I learned so much about all kind of different things, including research in general, RIXS and ARPES, quantum materials and electronic correlations, but also different cultures, countries and administrations. Much of what I learned, if not all, is owed to the many people I met and who guided me through the years.

First of all I want to thank my supervisors Johan Chang and Yasmine Sassa, who made this project possible in the first place. They were extremely supportive from the very start and helped navigating this project through both of their groups, never letting anything dim their positive attitude. Their support did not only include scientific aspects, but also additional, tedious administrative work for the arrangement of this jointly supervised PhD degree (or Double Doctoral Degree according to Chalmers, or Cotutelle de Thèse according to UZH) and personal advice on any kind of life situation. Their dedication to the students and their personal development is exceptional. I am most grateful for all the honest and open discussions, for bearing with my scepticism and always finding a new way to encourage me. I always felt appreciated and free to bring in my own opinion and ideas.

During the annual PhD meetings I profited from fruitful discussions with Elizabeth Blackburn and Fabian Natterer, who guided my projects with good questions and suggestions. My thanks also go to Aleksandar Matic, my examiner at Chalmers, and Lars Börjesson, my assistant supervisor. Concerning the special graduation procedure of my jointly supervised degree and concomitant extra efforts, I thank Laurent Duda, Hugo Dil, Thomas Greber and Laura Chaix for being part of the external committee and Giacomo Ghiringhelli for being my opponent.

My experiments would have not been possible without the effort of all the beamline scientists, welcoming the users and providing support and help. During all my travels to different synchrotrons, I learned early on that these scientists do not only provide the community with state-of-the-art endstations, but also with a deep knowledge in measurement techniques, various scientific areas, compound families and physical concepts, as well as good advice on local restaurants, customs and the intricate politics of science and largescale facilities. My thanks go to all the staff of both RIXS and ARPES beamlines I visited: ADRESS, SIS, I21, I05, ID32 and BLOCH.

Special thanks go to: Thorsten Schmitt for taking the time to introduce me to RIXS and answer all my questions; to Mirian Garcia-Fernandez for funny, interesting and comforting discussions and the most welcoming atmosphere in a beamline hutch; to Craig Polley for insightful discussions about ARPES, Python and scarce food options at MaxIV; and to Ke-Jin Zhou, Stefano Agrestini, Nick Plumb, Balasubramanian Thiagarajan, Nicholas Brookes and Davide Betto for most valuable support.

The rich excitation spectrum on Ca_2RuO_4 and $Ca_3Ru_2O_7$ would have never made sense to me without the support from Mario Cuoco and Fiona Forte. They not only provided the model calculations and theoretical interpretation, but also helped me with countless and fruitful discussions, patient explanations and an overall great collaboration.

Very heartfelt thanks go to Milan Radovic and Alla Chikina, who introduced me to the art of thin film growth and made the $LiTi_2O_4$ project not only possible, but also successful. I enjoyed all the informative, didactic discussions about science, but even more the many discussions outside of science, about politics, cultures and mushrooms.

In the first two and a half years that I spent at UZH in Zürich, I was lucky to work in the group of Johan Chang, where I was supported by so many people. I want to thank all the former and current members of the Laboratory for Quantum Matter Research group that I happened to meet. Special thanks go to Masafumi Horio, for patiently introducing me to all the aspects of RIXS and always finding the time to answer my numerous questions. My deepest thanks also go to Qisi Wang, who took over the part of getting hundreds of questions after Masafumi had left. I can't put words to how grateful I am to have worked with him, he is not only a patient and dedicated teacher, but a wonderful teammate and great scientist. There was nothing I couldn't ask and his advice was always most valuable. Next, I want to thank Kevin Kramer, sharing an office and going on beamtimes together was always peaceful and enjoyable. I specially thank him for great discussions about Python, teaching and train travels, I learned more than I could have hoped for. I am also thankful to Julia Küspert and Chun Lin, not only for sharing the office and many beamtime hours, but also for enriching discussions and advice. Whenever I happened to enter the lab or seeking any kind of technical advice, I was most happy to find Dominik Biscette, Denys Sutter and Damian Bucher, as they could always help by knowing where things are, coming up with a solution, an entertaining story or a good joke. Many thanks go to Jaewon Choi, who shared the most challenging but at the same time most amazing travel with me, guided and supported me in many ways and was always ready to help, not only as a teammate, but also as a friend. Of course, my deepest thanks also go to my dear Lakshmi Das, for all the wonderful and crazy times we have spent together, for making me laugh until I cried, for making

conferences and schools most enjoyable, and for sharing stories and friendship. For being a great Master student I would like to thank Pascal Rothenbühler, who I was trusted with to guide through his thesis project. I learned a lot myself along the way. Last but not least in this UZH section, I want to thank Matthias Hengsberger, who was the go-to person since my first day as a Bachelor student, well known to be able to solve any kind of problem. Starting from lab and teaching questions, over advice during my Bachelor thesis up to hands-on help during beamtimes and data analysis and interpretation, I could always count on him.

After my time at UZH, I moved to Göteborg for the last one and a half years with Yasmine Sassa's group at Chalmers. Although it was hard at first to leave my very familiar environment at UZH, I was welcomed so warmly by the whole Materials Physics division that I felt at home very soon. The closeness, friendliness and collegiality is most unique and appreciated. I want to thank everybody at the division for all the cozy Swedish fika breaks, the stories shared, the fun lunch breaks and entertaining afterworks. Many thanks go to the different office mates I had during my time at Chalmers: Yuqing Ge, Matthew Sadd, Matteo Palluzzi, Sofia Reiner and Elin Dufvenius Esping. They always cheered me up and created a comfy atmosphere. A special thanks also goes to my group colleagues Konstantinos Papadopoulos, again Yuqing Ge and Ola Forslund (he has to forgive me for putting him in this paragraph, he moved through all the extended group family during my PhD), who were with me in spirit, if not so often in person. In all the occasions we had together, was it a popular science presentation or beamtimes, they always made everything more fun and discussions about science were not only insightful, but also mind-broadening. In the extended family of collaborating groups, I also want to thank Ugne Miniotaite and Frank Elson for helping at beamtimes, bringing more laughter and also for sharing frustration as well as tips and tricks on how to survive a PhD. My thanks also go to Martin Månsson and Maëlys, for pleasent times in Stockholm and on beamtimes, discussions with both of them were always enjoyable and seeing them entering the hutch with lots of sweets to share can lift everyone's spirit.

My deepest thanks go out to my family and closest friends. Without their unconditional love and encouragment, I wouldn't have made it so far. They support me wherever I may be, through the good and bad times, and always believe in me; for this I am truly grateful. My final thank goes to Paolo Usai, who contributed to this work in so many different ways, but most importantly by keeping me sane throughout this crazy journey. His endless support and inspiration carried me through the hardest moments, and his love and warmth give me hope and strength.

References

[1] International year of basic sciences for development (2023). URL https://www.iybssd2022.org/en/home/.

[2] Bloch, F. Über die Quantenmechanik der Elektronen in Kristallgittern. *Z. Phys.* **52**, 555–600 (1929). URL https://doi.org/10.1007/BF01339455.

[3] Bardeen, J., Cooper, L. N. & Schrieffer, J. R. Microscopic Theory of Superconductivity. *Phys. Rev.* **106**, 162–164 (1957). URL https://link.aps.org/doi/10.1103/PhysRev.106.162.

[4] Lee, S., Kim, J.-H. & Kwon, Y.-W. The First Room-Temperature Ambient-Pressure Superconductor (2023). URL http://arxiv.org/abs/2307.12008.

[5] Garisto, D. LK-99 isn't a superconductor — how science sleuths solved the mystery. *Nature* **620**, 705–706 (2023). URL https://www.nature.com/articles/d41586-023-02585-7.

[6] Onnes, H. K. Further experiments with liquid helium. C. On the change of electric resistance of pure metals at very low temperatures etc. IV. The resistance of pure mercury at helium temperatures. In Onnes, H. K., Gavroglu, K. & Goudaroulis, Y. (eds.) *Through Measurement to Knowledge: The Selected Papers of Heike Kamerlingh Onnes 1853–1926*, Boston Studies in the Philosophy of Science, 261–263 (Springer Netherlands, Dordrecht, 1991). URL https://doi.org/10.1007/978-94-009-2079-8_15.

[7] Pickard, C. J., Errea, I. & Eremets, M. I. Superconducting Hydrides Under Pressure. *Annu. Rev. Condens. Matter Phys.* **11**, 57–76 (2020).

[8] Castelvecchi, D. How would room-temperature superconductors change science? *Nature* **621**, 18–19 (2023). URL https://www.nature.com/articles/d41586-023-02681-8.

[9] Keimer, B., Kivelson, S. A., Norman, M. R., Uchida, S. & Zaanen, J. From quantum matter to high-temperature superconductivity in copper oxides. *Nature* **518**, 179–186 (2015). URL https://www.nature.com/articles/nature14165.

[10] Dagotto, E. Complexity in Strongly Correlated Electronic Systems. *Science* **309**, 257–262 (2005). URL http://www.sciencemag.org/cgi/doi/10.1126/science.1107559.

[11] Knebel, G., Aoki, D. & Flouquet, J. Antiferromagnetism and superconductivity in cerium based heavy-fermion compounds. *C. R. Phys.* **12**, 542–566 (2011). URL https://www.sciencedirect.com/science/article/pii/S1631070511001204.

[12] Martinelli, A., Bernardini, F. & Massidda, S. The phase diagrams of iron-based superconductors: Theory and experiments. *C. R. Phys.* **17**, 5–35 (2016). URL https://www.sciencedirect.com/science/article/pii/S1631070515001267.

[13] Ament, L. J. P., van Veenendaal, M., Devereaux, T. P., Hill, J. P. & van den Brink, J. Resonant inelastic x-ray scattering studies of elementary excitations. *Rev. Mod. Phys.* **83**, 705–767 (2011). URL https://link.aps.org/doi/10.1103/RevModPhys.83.705.

[14] Sobota, J. A., He, Y. & Shen, Z.-X. Angle-resolved photoemission studies of quantum materials. *Rev. Mod. Phys.* **93**, 025006 (2021). URL https://link.aps.org/doi/10.1103/RevModPhys.93.025006.

[15] Shen, Z.-X., Lanzara, A., Ishihara, S. & Nagaosa, N. Role of the electron-phonon interaction in the strongly correlated cuprate superconductors. *Philos. Mag. B* **82**, 1349–1368 (2002). URL https://doi.org/10.1080/13642810208220725.

[16] Sutter, D. *et al.* Hallmarks of Hunds coupling in the Mott insulator Ca_2RuO_4. *Nat. Commun.* **8**, 15176 (2017). URL http://www.nature.com/articles/ncomms15176.

[17] Kotani, A. & Shin, S. Resonant inelastic x-ray scattering spectra for electrons in solids. *Rev. Mod. Phys.* **73**, 203–246 (2001). URL https://link.aps.org/doi/10.1103/RevModPhys.73.203.

[18] Åberg, T. Unified Theory of Auger Electron Emission. *Phys. Scr.* **1992**, 71 (1992). URL https://dx.doi.org/10.1088/0031-8949/1992/T41/013.

[19] de Groot, F. High-Resolution X-ray Emission and X-ray Absorption Spectroscopy. *Chem. Rev.* **101**, 1779–1808 (2001). URL https://pubs.acs.org/doi/10.1021/cr9900681.

[20] Minola, M. *Magnetic, Orbital and Charge Fluctuations in Layered Cuprates Studied by Resonant Soft X-Ray Scattering.* Ph.D. thesis, Politecnico di Milano (2013).

[21] Ament, L. J. P., Ghiringhelli, G., Sala, M. M., Braicovich, L. & van den Brink, J. Theoretical Demonstration of How the Dispersion of Magnetic Excitations in Cuprate Compounds can be Determined Using Resonant Inelastic X-Ray Scattering. *Phys. Rev. Lett.* **103**, 117003 (2009). URL https://link.aps.org/doi/10.1103/PhysRevLett.103.117003.

[22] Haverkort, M. W. Theory of Resonant Inelastic X-Ray Scattering by Collective Magnetic Excitations. *Phys. Rev. Lett.* **105**, 167404 (2010). URL https://link.aps.org/doi/10.1103/PhysRevLett.105.167404.

[23] Ament, L. J. P., van Veenendaal, M. v. & van den Brink, J. Determining the electron-phonon coupling strength from Resonant Inelastic X-ray Scattering at transition metal L-edges. *EPL* **95**, 27008 (2011). URL https://dx.doi.org/10.1209/0295-5075/95/27008.

[24] Braicovich, L. *et al.* Determining the electron-phonon coupling in superconducting cuprates by resonant inelastic x-ray scattering: Methods and results on $Nd_{1+x}Ba_{2-x}Cu_3O_{7-\delta}$. *Phys. Rev. Res.* **2**, 023231 (2020). URL https://link.aps.org/doi/10.1103/PhysRevResearch.2.023231.

[25] Zhou, K.-J. *et al.* I21: an advanced high-resolution resonant inelastic X-ray scattering beamline at Diamond Light Source. *J. Synchrotron Radiat.* **29**, 563–580 (2022). URL https://journals.iucr.org/s/issues/2022/02/00/rv5159/.

[26] Schmitt, T. *et al.* High-resolution resonant inelastic X-ray scattering with soft X-rays at the ADRESS beamline of the Swiss light source: Instrumental developments and scientific highlights. *J. Electron Spectrosc. Relat. Phenom.* **188**, 38–46 (2013). URL https://linkinghub.elsevier.com/retrieve/pii/S0368204813000030.

[27] Brookes, N. B. *et al.* The beamline ID32 at the ESRF for soft X-ray high energy resolution resonant inelastic X-ray scattering and polarisation dependent X-ray absorption spectroscopy. *Nucl. Instrum. Methods Phys. Res. A* **903**, 175–192 (2018). URL http://www.sciencedirect.com/science/article/pii/S0168900218308234.

[28] Penner-Hahn, J. E. 2.13 - X-ray Absorption Spectroscopy. In McCleverty, J. A. & Meyer, T. J. (eds.) *Comprehensive Coordination Chemistry II*, 159–186 (Pergamon, Oxford, 2003). URL https://www.sciencedirect.com/science/article/pii/B008043748601063X.

[29] Jöhr, S. *Removing Domain Boundaries in La_2CuO_4, $Ca_3Ru_2O_7$ and $YBa_2Cu_3O_{7-x}$ using a Thermo-Mechanical Detwinning Device*. Bachelor Thesis, Universität Zürich, Zürich (2019).

[30] Monney, C. *et al.* Resonant inelastic x-ray scattering study of the spin and charge excitations in the overdoped superconductor $La_{1.77}Sr_{0.23}CuO_4$. *Phys. Rev. B* **93**, 075103 (2016). URL https://link.aps.org/doi/10.1103/PhysRevB.93.075103.

[31] Hertz, H. *Ann. Phys.* **17**, 983 (1887).

[32] Einstein, A. Über einen die Erzeugung und Verwandlung des Lichtes betreffenden heuristischen Gesichtspunkt. *Ann. Phys.* **322**, 132–148 (1905). URL https://onlinelibrary.wiley.com/doi/abs/10.1002/andp.19053220607.

[33] Planck, M. Ueber das Gesetz der Energieverteilung im Normalspectrum. *Ann. Phys.* **309**, 553–563 (1901). URL https://onlinelibrary.wiley.com/doi/abs/10.1002/andp.19013090310.

[34] Damascelli, A. Probing the Electronic Structure of Complex Systems by ARPES. *Phys. Scr.* **2004**, 61 (2004). URL https://iopscience.iop.org/article/10.1238/Physica.Topical.109a00061/meta.

[35] Hüfner, S. *Very High Resolution Photoelectron Spectroscopy*. Lecture Notes in Physics Vol. 715 (Springer Berlin, Heidelberg, 2007).

[36] Kramer, K. P. *Illuminating Correlated Matter with Angle-Resolved Photoemission Spectroscopy*. Ph.D. thesis, Universität Zürich, Zürich (2022).

[37] Sutter, D. *Strong Electron Correlations in the Ruthenates*. Ph.D. thesis, Universität Zürich, Zürich (2019).

[38] Fermi, E. *Nuclear Physics: A Course Given by Enrico Fermi at the University of Chicago* (University of Chicago Press, Chicago, IL, 1974). URL https://press.uchicago.edu/ucp/books/book/chicago/N/bo3631242.html.

[39] Mahan, G. D. Theory of Photoemission in Simple Metals. *Phys. Rev. B* **2**, 4334–4350 (1970). URL https://link.aps.org/doi/10.1103/PhysRevB.2.4334.

[40] Berglund, C. N. & Spicer, W. E. Photoemission Studies of Copper and Silver: Theory. *Phys. Rev.* **136**, A1030–A1044 (1964). URL https://link.aps.org/doi/10.1103/PhysRev.136.A1030.

[41] Sassa, Y. *ARPES Investigations on in situ PLD grown $YBa_2Cu_3O_{7-\delta}$*. Ph.D. thesis, Université de Neuchâtel, Neuchâtel (2011).

[42] Hüfner, S. *Photoelectron Spectroscopy: Principles and Applications* (Springer Science & Business Media, 2013).

[43] Damascelli, A., Hussain, Z. & Shen, Z.-X. Angle-resolved photoemission studies of the cuprate superconductors. *Rev. Mod. Phys.* **75**, 473–541 (2003). URL https://link.aps.org/doi/10.1103/RevModPhys.75.473.

[44] SIS | SIS | Paul Scherrer Institut (PSI). URL https://www.psi.ch/en/sls/sis.

[45] DA30-L - Scienta Omicron. URL https://scientaomicron.com/en/Instruments/Electron-Analysers/DA30-L.

[46] Krebs, H.-U. *et al.* Pulsed Laser Deposition (PLD) – A Versatile Thin Film Technique. In Kramer, B. (ed.) *Advances in Solid State Physics, vol. 43*, 505–518 (Springer, Berlin, Heidelberg, 2003). URL https://doi.org/10.1007/978-3-540-44838-9_36.

[47] von Arx, K. *et al.* Resonant inelastic x-ray scattering study of $Ca_3Ru_2O_7$. *Phys. Rev. B* **102**, 235104 (2020). URL https://link.aps.org/doi/10.1103/PhysRevB.102.235104.

[48] von Arx, K. *et al.* Resolving the Orbital Character of Low-energy Excitations in Mott Insulator with Intermediate Spin-orbit Coupling. *Manuscript submitted to npj Quantum Mater., under review* (2023).

[49] Mott, N. F. The Basis of the Electron Theory of Metals, with Special Reference to the Transition Metals. *Proc. Phys. Soc. A* **62**, 416–422 (1949). URL http://stacks.iop.org/0370-1298/62/i=7/a=303?key=crossref.515afcc1de0314fd7d5fc679ef50eff4.

[50] Roy, S. B. Mott insulators and related phenomena: a basic introduction. In *Mott Insulators: Physics and Applications* (IOP Publishing, 2019). URL https://iopscience.iop.org/book/mono/978-0-7503-1596-8/chapter/bk978-0-7503-1596-8ch3.

[51] Maeno, Y. *et al.* Superconductivity in a layered perovskite without copper. *Nature* **372**, 532–534 (1994). URL https://www.nature.com/articles/372532a0.

[52] Fang, Z., Terakura, K. & Kanamori, J. Strong ferromagnetism and weak antiferromagnetism in double perovskites: Sr_2Fe*m*O_6 (*m*=Mo,W, and Re). *Phys. Rev. B* **63**, 180407 (2001). URL https://link.aps.org/doi/10.1103/PhysRevB.63.180407.

[53] Georges, A., Medici, L. d. & Mravlje, J. Strong Correlations from Hund's Coupling. *Annu. Rev. Condens. Matter Phys.* **4**, 137–178 (2013). URL http://www.annualreviews.org/doi/10.1146/annurev-conmatphys-020911-125045.

[54] Tokura, Y. & Nagaosa, N. Orbital Physics in Transition-Metal Oxides. *Science* **288**, 462–468 (2000). URL http://www.sciencemag.org/cgi/doi/10.1126/science.288.5465.462.

[55] Friedt, O. *et al.* Structural and magnetic aspects of the metal-insulator transition in $Ca_{2-x}Sr_xRuO_4$. *Phys. Rev. B* **63**, 174432 (2001). URL https://link.aps.org/doi/10.1103/PhysRevB.63.174432.

[56] Nakatsuji, S. & Maeno, Y. Quasi-Two-Dimensional Mott Transition System $Ca_{2-x}Sr_xRuO_4$. *Phys. Rev. Lett.* **84**, 2666–2669 (2000). URL https://link.aps.org/doi/10.1103/PhysRevLett.84.2666.

[57] Braden, M., André, G., Nakatsuji, S. & Maeno, Y. Crystal and magnetic structure of Ca_2RuO_4: Magnetoelastic coupling and the metal-insulator transition. *Phys. Rev. B* **58**, 847–861 (1998). URL https://link.aps.org/doi/10.1103/PhysRevB.58.847.

[58] Nobukane, H. *et al.* Co-appearance of superconductivity and ferromagnetism in a Ca_2RuO_4 nanofilm crystal. *Sci. Rep.* **10**, 3462 (2020). URL https://www.nature.com/articles/s41598-020-60313-x.

[59] Alireza, P. L. *et al.* Evidence of superconductivity on the border of quasi-2D ferromagnetism in Ca_2RuO_4 at high pressure. *J. Phys.: Condens. Matter* **22**, 052202 (2010). URL https://dx.doi.org/10.1088/0953-8984/22/5/052202.

[60] Jain, A. *et al.* Higgs mode and its decay in a two-dimensional antiferromagnet. *Nat. Phys.* **13**, 633–637 (2017). URL http://www.nature.com/articles/nphys4077.

[61] Souliou, S.-M. *et al.* Raman Scattering from Higgs Mode Oscillations in the Two-Dimensional Antiferromagnet Ca_2RuO_4. *Phys. Rev. Lett.* **119**, 067201 (2017). URL http://link.aps.org/doi/10.1103/PhysRevLett.119.067201.

[62] Xing, H. *et al.* Existence of electron and hole pockets and partial gap opening in the correlated semimetal $Ca_3Ru_2O_7$. *Phys. Rev. B* **97**, 041113 (2018). URL https://link.aps.org/doi/10.1103/PhysRevB.97.041113.

[63] Yoshida, Y. *et al.* Crystal and magnetic structure of $Ca_3Ru_2O_7$. *Phys. Rev. B* **72**, 054412 (2005). URL https://link.aps.org/doi/10.1103/PhysRevB.72.054412.

[64] Cao, G., McCall, S., Crow, J. E. & Guertin, R. P. Observation of a Metallic Antiferromagnetic Phase and Metal to Nonmetal Transition in $Ca_3Ru_2O_7$. *Phys. Rev. Lett.* **78**, 1751–1754 (1997). URL https://link.aps.org/doi/10.1103/PhysRevLett.78.1751.

[65] Zhu, M. *et al.* Colossal Magnetoresistance in a Mott Insulator via Magnetic Field-Driven Insulator-Metal Transition. *Phys. Rev. Lett.* **116**, 216401 (2016). URL https://link.aps.org/doi/10.1103/PhysRevLett.116.216401.

[66] Nelson, C. S. *et al.* Spin-charge-lattice coupling near the metal-insulator transition in $Ca_3Ru_2O_7$. *Phys. Rev. B* **75**, 212403 (2007). URL https://link.aps.org/doi/10.1103/PhysRevB.75.212403.

[67] Yoshida, Y. *et al.* Quasi-two-dimensional metallic ground state of $Ca_3Ru_2O_7$. *Phys. Rev. B* **69**, 220411 (2004). URL https://link.aps.org/doi/10.1103/PhysRevB.69.220411.

[68] Cao, G., Balicas, L., Xin, Y., Crow, J. E. & Nelson, C. S. Quantum oscillations, colossal magnetoresistance, and the magnetoelastic interaction in bilayered $Ca_3Ru_2O_7$. *Phys. Rev. B* **67**, 184405 (2003). URL https://link.aps.org/doi/10.1103/PhysRevB.67.184405.

[69] Baumberger, F. *et al.* Nested Fermi Surface and Electronic Instability in $Ca_3Ru_2O_7$. *Phys. Rev. Lett.* **96**, 107601 (2006). URL https://link.aps.org/doi/10.1103/PhysRevLett.96.107601.

[70] Lin, X. N., Zhou, Z. X., Durairaj, V., Schlottmann, P. & Cao, G. Colossal Magnetoresistance by Avoiding a Ferromagnetic State in the Mott System $Ca_3Ru_2O_7$. *Phys. Rev. Lett.* **95**, 017203 (2005). URL https://link.aps.org/doi/10.1103/PhysRevLett.95.017203.

[71] Fatuzzo, C. G. *et al.* Spin-orbit-induced orbital excitations in Sr_2RuO_4 and Ca_2RuO_4: A resonant inelastic x-ray scattering study. *Phys. Rev. B* **91**, 155104 (2015). URL https://link.aps.org/doi/10.1103/PhysRevB.91.155104.

[72] Das, L. *et al.* Spin-Orbital Excitations in Ca_2RuO_4 Revealed by Resonant Inelastic X-Ray Scattering. *Phys. Rev. X* **8**, 011048 (2018). URL https://link.aps.org/doi/10.1103/PhysRevX.8.011048.

[73] Zegkinoglou, I. *et al.* Orbital Ordering Transition in Ca_2RuO_4 Observed with Resonant X-Ray Diffraction. *Phys. Rev. Lett.* **95**, 136401 (2005). URL https://link.aps.org/doi/10.1103/PhysRevLett.95.136401.

[74] Suzuki, H. *et al.* Spin waves and spin-state transitions in a ruthenate high-temperature antiferromagnet. *Nat. Mater.* **18**, 563–567 (2019). URL http://arxiv.org/abs/1904.01930.

[75] Fukazawa, H., Nakatsuji, S. & Maeno, Y. Intrinsic properties of the Mott insulator $Ca_2RuO_{4+\delta}$ (δ=0) studied with single crystals. *Physica B: Condens. Matter* **281-282**, 613 – 614 (2000). URL http://www.sciencedirect.com/science/article/pii/S0921452699009898.

[76] Nakatsuji, S. & Maeno, Y. Synthesis and Single-Crystal Growth of $Ca_{2-x}Sr_xRuO_4$. *J. Solid State Chem.* **156**, 26–31 (2001). URL https://linkinghub.elsevier.com/retrieve/pii/S0022459600989539.

[77] Sala, M. M. *et al.* Orbital occupancies and the putative $j_{eff} = 1/2$ ground state in Ba_2IrO_4: A combined oxygen K-edge XAS and RIXS study. *Phys. Rev. B* **89**, 121101 (2014). URL https://link.aps.org/doi/10.1103/PhysRevB.89.121101.

[78] Chen, C. T. *et al.* Out-of-plane orbital characters of intrinsic and doped holes in $La_{2-x}Sr_xCuO_4$. *Phys. Rev. Lett.* **68**, 2543–2546 (1992). URL https://link.aps.org/doi/10.1103/PhysRevLett.68.2543.

[79] Malvestuto, M. *et al.* Electronic structure trends in the $Sr_{n+1}Ru_nO_{3n+1}$ family ($n = 1, 2, 3$). *Phys. Rev. B* **83**, 165121 (2011). URL https://link.aps.org/doi/10.1103/PhysRevB.83.165121.

[80] Malvestuto, M. *et al.* Nature of the apical and planar oxygen bonds in the $Sr_{n+1}Ru_nO_{3n+1}$ family ($n = 1, 2, 3$). *Phys. Rev. B* **88**, 195143 (2013). URL https://link.aps.org/doi/10.1103/PhysRevB.88.195143.

[81] Guedes, E. B. *et al.* Core level and valence band spectroscopy of $SrRuO_3$: Electron correlation and covalence effects. *Phys. Rev. B* **86**, 235127 (2012). URL https://link.aps.org/doi/10.1103/PhysRevB.86.235127.

[82] Braden, M., Reichardt, W., Sidis, Y., Mao, Z. & Maeno, Y. Lattice dynamics and electron-phonon coupling in Sr_2RuO_4 : Inelastic neutron scattering and

shell-model calculations. *Phys. Rev. B* **76**, 014505 (2007). URL https://link.aps.org/doi/10.1103/PhysRevB.76.014505.

[83] Cuoco, M., Forte, F. & Noce, C. Probing spin-orbital-lattice correlations in $4d^4$ systems. *Phys. Rev. B* **73**, 094428 (2006). URL https://link.aps.org/doi/10.1103/PhysRevB.73.094428.

[84] Cuoco, M., Forte, F. & Noce, C. Interplay of Coulomb interactions and c-axis octahedra distortions in single-layer ruthenates. *Phys. Rev. B* **74**, 195124 (2006). URL https://link.aps.org/doi/10.1103/PhysRevB.74.195124.

[85] Ament, L. J. P., Forte, F. & van den Brink, J. Ultrashort lifetime expansion for indirect resonant inelastic x-ray scattering. *Phys. Rev. B* **75**, 115118 (2007). URL https://link.aps.org/doi/10.1103/PhysRevB.75.115118.

[86] Dean, M. P. M. *et al.* Persistence of magnetic excitations in $La_{2-x}Sr_xCuO_4$ from the undoped insulator to the heavily overdoped non-superconducting metal. *Nat. Mater.* **12**, 1019–1023 (2013). URL https://www.nature.com/articles/nmat3723.

[87] Pelliciari, J. *et al.* Reciprocity between local moments and collective magnetic excitations in the phase diagram of $BaFe_2(As_{1-x}P_x)_2$. *Commun. Phys.* **2**, 139 (2019). URL http://www.nature.com/articles/s42005-019-0236-3.

[88] House, R. A. *et al.* Covalency does not suppress O_2 formation in 4d and 5d Li-rich O-redox cathodes. *Nat. Commun.* **12**, 2975 (2021). URL https://www.nature.com/articles/s41467-021-23154-4.

[89] Kim, J. *et al.* Magnetic Excitation Spectra of Sr_2IrO_4 Probed by Resonant Inelastic X-Ray Scattering: Establishing Links to Cuprate Superconductors. *Phys. Rev. Lett.* **108**, 177003 (2012). URL https://link.aps.org/doi/10.1103/PhysRevLett.108.177003.

[90] Kim, J. *et al.* Excitonic quasiparticles in a spin–orbit Mott insulator. *Nat. Commun.* **5**, 4453 (2014). URL https://www.nature.com/articles/ncomms5453.

[91] Paris, E. *et al.* Strain engineering of the charge and spin-orbital interactions in Sr_2IrO_4. *Proc. Natl. Acad. Sci. USA* **117**, 24764–24770 (2020). URL https://www.pnas.org/doi/full/10.1073/pnas.2012043117.

[92] Geondzhian, A. *et al.* Large Polarons as Key Quasiparticles in $SrTiO_3$ and $SrTiO_3$-Based Heterostructures. *Phys. Rev. Lett.* **125**, 126401 (2020). URL https://link.aps.org/doi/10.1103/PhysRevLett.125.126401.

[93] Wang, Q. *et al.* Charge order lock-in by electron-phonon coupling in $La_{1.675}Eu_{0.2}Sr_{0.125}CuO_4$. *Sci. Adv.* **7**, eabg7394 (2021). URL https://advances.sciencemag.org/content/7/27/eabg7394.

[94] Vale, J. G. *et al.* High-resolution resonant inelastic x-ray scattering study of the electron-phonon coupling in honeycomb $\alpha - Li_2IrO_3$. *Phys. Rev. B* **100**, 224303 (2019). URL https://link.aps.org/doi/10.1103/PhysRevB.100.224303.

[95] Gretarsson, H. *et al.* Observation of spin-orbit excitations and Hund's multiplets in Ca_2RuO_4. *Phys. Rev. B* **100**, 045123 (2019). URL https://link.aps.org/doi/10.1103/PhysRevB.100.045123.

[96] Bednorz, J. G. & Müller, K. A. Possible high t_c superconductivity in the Ba–La–Cu–O system. *Z. Phys. B - Condens. Matter* **64**, 189–193 (1986). URL https://doi.org/10.1007/BF01303701.

[97] Dai, P. *et al.* Synthesis and neutron powder diffraction study of the superconductor $HgBa_2Ca_2Cu_3O_{8+\delta}$ by Tl substitution. *Physica C: Supercond.* **243**, 201–206 (1995). URL https://www.sciencedirect.com/science/article/pii/0921453494024618.

[98] Wang, Q. *et al.* High-Temperature Charge-Stripe Correlations in $La_{1.675}Eu_{0.2}Sr_{0.125}CuO_4$. *Phys. Rev. Lett.* **124**, 187002 (2020). URL https://link.aps.org/doi/10.1103/PhysRevLett.124.187002.

[99] von Arx, K. *et al.* Fate of charge order in overdoped La-based cuprates. *npj Quantum Mater.* **8**, 1–6 (2023). URL https://www.nature.com/articles/s41535-023-00539-w.

[100] Matt, C. E. *et al.* Direct observation of orbital hybridisation in a cuprate superconductor. *Nat. Commun.* **9**, 972 (2018). URL https://www.nature.com/articles/s41467-018-03266-0.

[101] Tallon, J. L., Storey, J. G., Cooper, J. R. & Loram, J. W. Locating the pseudogap closing point in cuprate superconductors: Absence of entrant or reentrant behavior. *Phys. Rev. B* **101**, 174512 (2020). URL https://link.aps.org/doi/10.1103/PhysRevB.101.174512.

[102] Daou, R. *et al.* Linear temperature dependence of resistivity and change in the Fermi surface at the pseudogap critical point of a high-t_c superconductor. *Nat. Phys.* **5**, 31–34 (2009). URL https://www.nature.com/articles/nphys1109.

[103] Cyr-Choinière, O. *et al.* Pseudogap temperature t^* of cuprate superconductors from the Nernst effect. *Phys. Rev. B* **97**, 064502 (2018). URL https://link.aps.org/doi/10.1103/PhysRevB.97.064502.

[104] Horio, M. *et al.* Three-Dimensional Fermi Surface of Overdoped La-Based Cuprates. *Phys. Rev. Lett.* **121**, 077004 (2018). URL https://link.aps.org/doi/10.1103/PhysRevLett.121.077004.

[105] Michon, B. *et al.* Thermodynamic signatures of quantum criticality in cuprate superconductors. *Nature* **567**, 218–222 (2019). URL https://www.nature.com/articles/s41586-019-0932-x.

[106] Gupta, N. K. *et al.* Vanishing nematic order beyond the pseudogap phase in overdoped cuprate superconductors. *Proc. Natl. Acad. Sci. USA* **118** (2021). URL https://www.pnas.org/content/118/34/e2106881118.

[107] Frachet, M. *et al.* Hidden magnetism at the pseudogap critical point of a cuprate superconductor. *Nat. Phys.* **16**, 1064–1068 (2020). URL https://www.nature.com/articles/s41567-020-0950-5.

[108] Tranquada, J. M., Sternlieb, B. J., Axe, J. D., Nakamura, Y. & Uchida, S. Evidence for stripe correlations of spins and holes in copper oxide superconductors. *Nature* **375**, 561–563 (1995). URL https://www.nature.com/articles/375561a0.

[109] Arpaia, R. & Ghiringhelli, G. Charge Order at High Temperature in Cuprate Superconductors. *J. Phys. Soc. Jpn.* **90**, 111005 (2021). URL https://journals.jps.jp/doi/10.7566/JPSJ.90.111005.

[110] Ghiringhelli, G. *et al.* Long-Range Incommensurate Charge Fluctuations in (Y,Nd)Ba2Cu3O6+x. *Science* **337**, 821–825 (2012). URL http://www.sciencemag.org/cgi/doi/10.1126/science.1223532.

[111] Ma, Q. *et al.* Parallel spin stripes and their coexistence with superconducting ground states at optimal and high doping in $La_{1.6-x}Nd_{0.4}Sr_xCuO_4$. *Phys. Rev. Res.* **3**, 023151 (2021). URL https://link.aps.org/doi/10.1103/PhysRevResearch.3.023151.

[112] Fujita, M., Goka, H., Yamada, K., Tranquada, J. M. & Regnault, L. P. Stripe order, depinning, and fluctuations in $La_{1.875}Ba_{0.125}CuO_4$ and $La_{1.875}Ba_{0.075}Sr_{0.050}CuO_4$. *Phys. Rev. B* **70**, 104517 (2004). URL https://link.aps.org/doi/10.1103/PhysRevB.70.104517.

[113] Hücker, M. *et al.* Spontaneous Symmetry Breaking by Charge Stripes in the High Pressure Phase of Superconducting $La_{1.875}Ba_{0.125}CuO_4$. *Phys. Rev. Lett.* **104**, 057004 (2010). URL https://link.aps.org/doi/10.1103/PhysRevLett.104.057004.

[114] Miao, H. *et al.* High-temperature charge density wave correlations in $La_{1.875}Ba_{0.125}CuO_4$ without spin–charge locking. *Proc. Natl. Acad. Sci. USA* **114**, 12430–12435 (2017). URL https://www.pnas.org/content/114/47/12430.

[115] Achkar, A. J. *et al.* Nematicity in stripe-ordered cuprates probed via resonant x-ray scattering. *Science* **351**, 576–578 (2016). URL https://www.sciencemag.org/lookup/doi/10.1126/science.aad1824.

[116] Fink, J. *et al.* Charge ordering in $La_{1.8-x}Eu_{0.2}Sr_xCuO_4$ studied by resonant soft x-ray diffraction. *Phys. Rev. B* **79**, 100502 (2009). URL https://link.aps.org/doi/10.1103/PhysRevB.79.100502.

[117] Fink, J. *et al.* Phase diagram of charge order in $La_{1.8-x}Eu_{0.2}Sr_xCuO_4$ from resonant soft x-ray diffraction. *Phys. Rev. B* **83**, 092503 (2011). URL https://link.aps.org/doi/10.1103/PhysRevB.83.092503.

[118] Peng, Y. *et al.* Enhanced Electron-Phonon Coupling for Charge-Density-Wave Formation in $La_{1.8-x}Eu_{0.2}Sr_xCuO_{4+\delta}$. *Phys. Rev. Lett.* **125**, 097002 (2020). URL https://link.aps.org/doi/10.1103/PhysRevLett.125.097002.

[119] Chang, J. *et al.* Direct observation of competition between superconductivity and charge density wave order in $YBa_2Cu_3O_{6.67}$. *Nat. Phys.* **8**, 871–876 (2012). URL https://www.nature.com/articles/nphys2456.

[120] Chang, J. *et al.* Nernst and Seebeck Coefficients of the Cuprate Superconductor $YBa_2Cu_3O_{6.67}$: A Study of Fermi Surface Reconstruction. *Phys. Rev. Lett.* **104**, 057005 (2010). URL https://link.aps.org/doi/10.1103/PhysRevLett.104.057005.

[121] Laliberté, F. *et al.* Fermi-surface reconstruction by stripe order in cuprate superconductors. *Nat. Commun.* **2**, 432 (2011). URL https://www.nature.com/articles/ncomms1440.

[122] Peng, Y. Y. *et al.* Re-entrant charge order in overdoped $(Bi,Pb)_{2.12}Sr_{1.88}CuO_{6+\delta}$ outside the pseudogap regime. *Nat. Mater.* **17**, 697–702 (2018). URL https://www.nature.com/articles/s41563-018-0108-3.

[123] Lin, J. *et al.* Strongly Correlated Charge Density Wave in $La_{2-x}Sr_xCuO_4$ Evidenced by Doping-Dependent Phonon Anomaly. *Phys. Rev. Lett.* **124**, 207005 (2020). URL https://link.aps.org/doi/10.1103/PhysRevLett.124.207005.

[124] Miao, H. *et al.* Charge density waves in cuprate superconductors beyond the critical doping. *npj Quantum Mater.* **6**, 1–6 (2021). URL https://www.nature.com/articles/s41535-021-00327-4.

[125] Wen, J.-J. *et al.* Observation of two types of charge-density-wave orders in superconducting $La_{2-x}Sr_xCuO_4$. *Nat. Commun.* **10**, 3269 (2019). URL https://www.nature.com/articles/s41467-019-11167-z.

[126] Brookes, N. *et al.* Stability of the Zhang-Rice Singlet with Doping in Lanthanum Strontium Copper Oxide Across the Superconducting Dome and Above. *Phys. Rev. Lett.* **115**, 027002 (2015). URL https://link.aps.org/doi/10.1103/PhysRevLett.115.027002.

[127] Chang, J. *et al.* Tuning competing orders in $La_{2-x}Sr_xCuO_4$ cuprate superconductors by the application of an external magnetic field. *Phys. Rev. B* **78**, 104525 (2008). URL https://link.aps.org/doi/10.1103/PhysRevB.78.104525.

[128] Lee, S. *et al.* Generic character of charge and spin density waves in superconducting cuprates. *Proc. Natl. Acad. Sci. USA* **119**, e2119429119 (2022). URL https://www.pnas.org/doi/full/10.1073/pnas.2119429119.

[129] Fang, Y. *et al.* Fermi surface transformation at the pseudogap critical point of a cuprate superconductor. *Nat. Phys.* **18**, 558–564 (2022). URL https://www.nature.com/articles/s41567-022-01514-1.

[130] Huang, H. *et al.* Quantum Fluctuations of Charge Order Induce Phonon Softening in a Superconducting Cuprate. *Phys. Rev. X* **11**, 041038 (2021). URL https://link.aps.org/doi/10.1103/PhysRevX.11.041038.

[131] Arpaia, R. *et al.* Dynamical charge density fluctuations pervading the phase diagram of a Cu-based high-Tc superconductor. *Science* **365**, 906–910 (2019). URL https://science.sciencemag.org/content/365/6456/906.

[132] Banerjee, S., Atkinson, W. A. & Kampf, A. P. Emergent charge order from correlated electron-phonon physics in cuprates. *Commun. Phys.* **3**, 1–8 (2020). URL https://www.nature.com/articles/s42005-020-00430-1.

[133] Li, Q. *et al.* Prevailing Charge Order in Overdoped $La_{2-x}Sr_xCuO_4$ beyond the Superconducting Dome. *Phys. Rev. Lett.* **131**, 116002 (2023). URL https://link.aps.org/doi/10.1103/PhysRevLett.131.116002.

[134] Zaanen, J. & Gunnarsson, O. Charged magnetic domain lines and the magnetism of high-t_c oxides. *Phys. Rev. B* **40**, 7391–7394 (1989). URL https://link.aps.org/doi/10.1103/PhysRevB.40.7391.

[135] Machida, K. Magnetism in La_2CuO_4 based compounds. *Physica C: Supercond.* **158**, 192–196 (1989). URL https://www.sciencedirect.com/science/article/pii/092145348990316X.

[136] Zhu, X., Cao, Y., Zhang, J., Plummer, E. W. & Guo, J. Classification of charge density waves based on their nature. *Proc. Natl. Acad. Sci. USA* **112**, 2367–2371 (2015). URL https://www.pnas.org/doi/10.1073/pnas.1424791112.

[137] Devereaux, T. *et al.* Directly Characterizing the Relative Strength and Momentum Dependence of Electron-Phonon Coupling Using Resonant Inelastic X-Ray Scattering. *Phys. Rev. X* **6**, 041019 (2016). URL https://link.aps.org/doi/10.1103/PhysRevX.6.041019.

[138] Reznik, D. *et al.* Electron–phonon coupling reflecting dynamic charge inhomogeneity in copper oxide superconductors. *Nature* **440**, 1170–1173 (2006). URL https://www.nature.com/articles/nature04704.

[139] Fukuda, T. *et al.* Doping dependence of softening in the bond-stretching phonon mode of $La_{2-x}Sr_xCuO_4$ ($0 \leq x \leq 0.29$). *Phys. Rev. B* **71**, 060501 (2005). URL https://link.aps.org/doi/10.1103/PhysRevB.71.060501.

[140] Giustino, F., Cohen, M. L. & Louie, S. G. Small phonon contribution to the photoemission kink in the copper oxide superconductors. *Nature* **452**, 975–978 (2008). URL https://www.nature.com/articles/nature06874.

[141] Falter, C., Bauer, T. & Schnetgöke, F. Modeling the electronic state of the high-t_c superconductor LaCuO: Phonon dynamics and charge response. *Phys. Rev. B* **73**, 224502 (2006). URL https://link.aps.org/doi/10.1103/PhysRevB.73.224502.

[142] Chaix, L. *et al.* Dispersive charge density wave excitations in $Bi_2Sr_2CaCu_2O_{8+\delta}$. *Nat. Phys.* **13**, 952–956 (2017). URL https://www.nature.com/articles/nphys4157.

[143] Lee, W. S. *et al.* Spectroscopic fingerprint of charge order melting driven by quantum fluctuations in a cuprate. *Nat. Phys.* **17**, 53–57 (2021). URL https://www.nature.com/articles/s41567-020-0993-7.

[144] Thampy, V. *et al.* Rotated stripe order and its competition with superconductivity in $La_{1.88}Sr_{0.12}CuO_4$. *Phys. Rev. B* **90**, 100510 (2014). URL https://link.aps.org/doi/10.1103/PhysRevB.90.100510.

[145] Johnston, D. C., Prakash, H., Zachariasen, W. H. & Viswanathan, R. High temperature superconductivity in the Li-Ti-O ternary system. *Mater. Res.*

Bull. **8**, 777–784 (1973). URL https://www.sciencedirect.com/science/article/pii/0025540873901839.

[146] Sugiyama, J. *et al.* Li-ion diffusion in $Li_4Ti_5O_{12}$ and $LiTi_2O_4$ battery materials detected by muon spin spectroscopy. *Phys. Rev. B* **92**, 014417 (2015). URL https://link.aps.org/doi/10.1103/PhysRevB.92.014417.

[147] Ohsawa, T. *et al.* Origin of Optical Transparency in a Transparent Superconductor $LiTi_2O_4$. *ACS Appl. Electron. Mater.* **2**, 517–522 (2020). URL https://doi.org/10.1021/acsaelm.9b00751.

[148] Inukai, T., Murakami, T. & Inamura, T. Preparation of superconducting $LiTi_2O_4$ thin films. *Thin Solid Films* **94**, 47–50 (1982). URL https://www.sciencedirect.com/science/article/pii/0040609082900281.

[149] Kumatani, A. *et al.* Growth processes of lithium titanate thin films deposited by using pulsed laser deposition. *Appl. Phys. Lett.* **101**, 123103 (2012). URL https://doi.org/10.1063/1.4752466.

[150] von Arx, K. *et al.* Evidence of strong electron correlations in the spinel superconductor $LiTi_2O_4$. *Manuscript in preparation* (2023).

[151] Ekino, T. & Akimitsu, J. Superconducting energy gap in spinel compound $Li_{1+x}Ti_{2-x}O_4$ from electron tunneling. *Physica B: Condens. Matter* **165-166**, 1599–1600 (1990). URL https://www.sciencedirect.com/science/article/pii/S0921452609803852.

[152] Anderson, P. W., Baskaran, G., Zou, Z. & Hsu, T. Resonating–valence-bond theory of phase transitions and superconductivity in La_2cuo_4-based compounds. *Phys. Rev. Lett.* **58**, 2790–2793 (1987). URL https://link.aps.org/doi/10.1103/PhysRevLett.58.2790.

[153] Satpathy, S. & Martin, R. M. Electronic structure of the superconducting oxide spinel $LiTi_2O_4$. *Phys. Rev. B* **36**, 7269–7272 (1987). URL https://link.aps.org/doi/10.1103/PhysRevB.36.7269.

[154] Alexandrov, A. & Ranninger, J. Bipolaronic superconductivity. *Phys. Rev. B* **24**, 1164–1169 (1981). URL https://link.aps.org/doi/10.1103/PhysRevB.24.1164.

[155] Jin, K. *et al.* Anomalous magnetoresistance in the spinel superconductor $LiTi_2O_4$. *Nat. Commun.* **6**, 7183 (2015). URL https://www.nature.com/articles/ncomms8183.

[156] Xue, H. *et al.* Fourfold Symmetric Superconductivity in Spinel Oxide $LiTi_2O_4$(001) Thin Films. *ACS Nano* **16**, 19464–19471 (2022). URL https://doi.org/10.1021/acsnano.2c09338.

[157] Nocerino, E. *et al.* Superconducting Properties of the Thin Film $LiTi_2O_4$ Spinel Compound Investigated by Low-Energy μ^+SR. *to be submitted to Commun. Phys.* (2023).

[158] Edwards, P. P. *et al.* A study of the spinel materials $LiTi_2O_4$ and $Li_{4/3}Ti_{5/3}O_4$ by photoelectron spectroscopy. *J. Solid State Chem.* **54**, 127–135 (1984). URL https://www.sciencedirect.com/science/article/pii/0022459684901403.

[159] Chen, C. L. *et al.* Role of 3d electrons in the rapid suppression of superconductivity in the dilute V doped spinel superconductor $LiTi_2O_4$. *Supercond. Sci. Technol.* **24**, 115007 (2011). URL https://dx.doi.org/10.1088/0953-2048/24/11/115007.

[160] Okada, Y. *et al.* Scanning tunnelling spectroscopy of superconductivity on surfaces of $LiTi_2O_4$(111) thin films. *Nat. Commun.* **8**, 15975 (2017). URL https://www.nature.com/articles/ncomms15975.

[161] Hengsberger, M., Frésard, R., Purdie, D., Segovia, P. & Baer, Y. Electron-phonon coupling in photoemission spectra. *Phys. Rev. B* **60**, 10796–10802 (1999). URL https://link.aps.org/doi/10.1103/PhysRevB.60.10796.

[162] Kordyuk, A. A. *et al.* Bare electron dispersion from experiment: Self-consistent self-energy analysis of photoemission data. *Phys. Rev. B* **71**, 214513 (2005). URL https://link.aps.org/doi/10.1103/PhysRevB.71.214513.

[163] Massidda, S., Yu, J. & Freeman, A. J. Electronic structure and properties of superconducting $LiTi_2O_4$. *Phys. Rev. B* **38**, 11352–11357 (1988). URL https://link.aps.org/doi/10.1103/PhysRevB.38.11352.

[164] Sun, C. P. *et al.* Magnetic field dependence of low-temperature specific heat of the spinel oxide superconductor $LiTi_2O_4$. *Phys. Rev. B* **70**, 054519 (2004). URL https://link.aps.org/doi/10.1103/PhysRevB.70.054519.

[165] Brouet, V. *et al.* Measuring Fermi velocities with ARPES in narrow band systems: The case of layered cobaltates. *J. Electron Spectrosc. Relat. Phenom.* **185**, 146–151 (2012). URL https://www.sciencedirect.com/science/article/pii/S0368204812000436.

[166] Fujisawa, Y. *et al.* Imaging emergent exotic quasiparticle state in a frustrated transition metal oxide (2023). URL http://arxiv.org/abs/2306.06708.

[167] Wines, D., Xie, T. & Choudhary, K. Inverse Design of Next-Generation Superconductors Using Data-Driven Deep Generative Models. *J. Phys. Chem. Lett.* **14**, 6630–6638 (2023). URL https://doi.org/10.1021/acs.jpclett.3c01260.

[168] The Nobel Prize in Physics. URL https://www.nobelprize.org/prizes/physics/.